Direct three-dimensional imaging of polar ionospheric structures with the Resolute Bay Incoherent Scatter Radar

H. Dahlgren,[1] J. L. Semeter,[1] K. Hosokawa,[2] M. J. Nicolls,[3] T. W. Butler,[1] M. G. Johnsen,[4,5] K. Shiokawa,[6] and C. Heinselman[3]

[1] Ionospheric plasma density structures in the dayside F-region of the polar cap are commonly occurring events, but adequate measurements of their formation and evolution have been sparse. With the advent of the advanced modular incoherent scatter radar RISR-N (Resolute Bay Incoherent Scatter Radar) it is now possible for the first time to study the temporal evolution of the plasma properties in the polar cap region in three dimensions, with a spatial resolution of tens of kilometers, from which the plasma rest frame can be experimentally established. We demonstrate the strength of the diagnostic with observations from an event of enhanced plasma density observed over Resolute Bay in December 2009. A colocated all-sky imager showed faint 630.0 and 557.7 nm emission corresponding to the plasma enhancements, and the structures could be traced back to a formation region in the open/closed field line boundary. This new plasma imaging technique will provide important information on the mechanisms controlling the structuring in the high latitude ionosphere. **Citation:** Dahlgren, H., J. L. Semeter, K. Hosokawa, M. J. Nicolls, T. W. Butler, M. G. Johnsen, K. Shiokawa, and C. Heinselman (2012), Direct three-dimensional imaging of polar ionospheric structures with the Resolute Bay Incoherent Scatter Radar, *Geophys. Res. Lett.*, *39*, L05104, doi:10.1029/2012GL050895.

1. Introduction

[2] The very high latitude ionosphere has been found to often contain a high degree of electron density structures with variations of at least a factor 2 during periods of southward IMF. The main physical processes behind the formation of such structures in the dayside polar cap region are plasma convection, auroral precipitation and solar photoionization, and their relative contribution has a profound effect on the characteristics of the enhancements. Poleward drifting optical features due to particle precipitation are also known as poleward moving auroral forms (PMAFs) [*Fasel*, 1995; *Sandholt et al.*, 1990]. The precipitation has its origin in transient reconnection at the magnetopause, from which newly opened flux tubes convect anti-sunward during what is known as a flux transfer event, FTEs [*Russell and Elphic*, 1978]. Good agreement has been observed between poleward drift of 630.0 nm optical enhancements and ionospheric flow channels [*Milan et al.*, 1999], and data from meridian scanning photometers have shown a decrease in the red line luminosity, and thus decrease of energy flux, as the structures move anti-sunward [*Sandholt and Farrugia*, 2007].

[3] Polar cap patches are regions of high-density plasma structures in the polar cap F-region, [e.g., *Weber et al.*, 1984; *Tsunoda*, 1988]. The 630.0 nm airglow emission intensity decays as the patches drift from their formation region in or near the cusp, anti-sunward with the background convection flow over the pole [*Hosokawa et al.*, 2011], with a typical speed in the range 100 to 1000 m/s [*Weber et al.*, 1984]. Polar cap patches can merge from regions of observed PMAFs [*Lorentzen et al.*, 2010] and they have been found to contain a high level of structuring, caused by small-scale plasma irregularities driven by plasma instabilities [*Basu et al.*, 1994; *Hosokawa et al.*, 2009]. *Oksavik et al.* [2010] also showed that patches deform and rotate during their passage over the polar cap, but very few measurements of ionospheric structures and their evolution are available in the polar cap region. Understanding their variability is an important factor in any modeling efforts of high latitude plasma.

[4] In this letter we evaluate the capabilities of the newly completed Advanced Modulated Incoherent Scatter Radar (AMISR) facility in Resolute Bay, and show for the first time a detailed image of the three dimensional distribution of plasma parameters such as the electron density in the deep polar cap region. By obtaining measurements in multiple directions simultaneously, it becomes possible to track density structures in the reference frame of the convecting plasma. This is critical for evaluating sources and sinks of high latitude plasma structures and to correctly estimate ionospheric heating rates, as pointed out by *Vasyliūnas and Song* [2005].

2. Instrumentation and Event Description

[5] The Resolute Bay Incoherent Scatter Radar (RISR-N) is a northward-looking, electronically steerable phased array antenna, located in Resolute Bay, Canada (74.7°N, 265.1°E, AACGM latitude 82.9°N), where it provides direct three dimensional measurements of the deep polar cap ionosphere [*Bahcivan et al.*, 2010]. The 480-μs long pulse experiment used in this study defines the range resolution to 72 km. The beam pointing direction is stepped through the 5 by 5 az/el

---

[1]Department of Electrical and Computer Engineering, Boston University, Boston, Massachusetts, USA.

[2]Department of Communication Engineering and Informatics, University of Electro-Communications, Chofu, Japan.

[3]SRI International, Menlo Park, California, USA.

[4]Department of Physics and Technology, University of Tromsø, Tromsø, Norway.

[5]Now at Tromsø Geophysical Observatory, University of Tromsø, Tromsø, Norway.

[6]Solar-Terrestrial Environment Laboratory, Nagoya University, Nagoya, Japan.

OMTI red and green channels overlayed

OMTI red channel with RISR contour
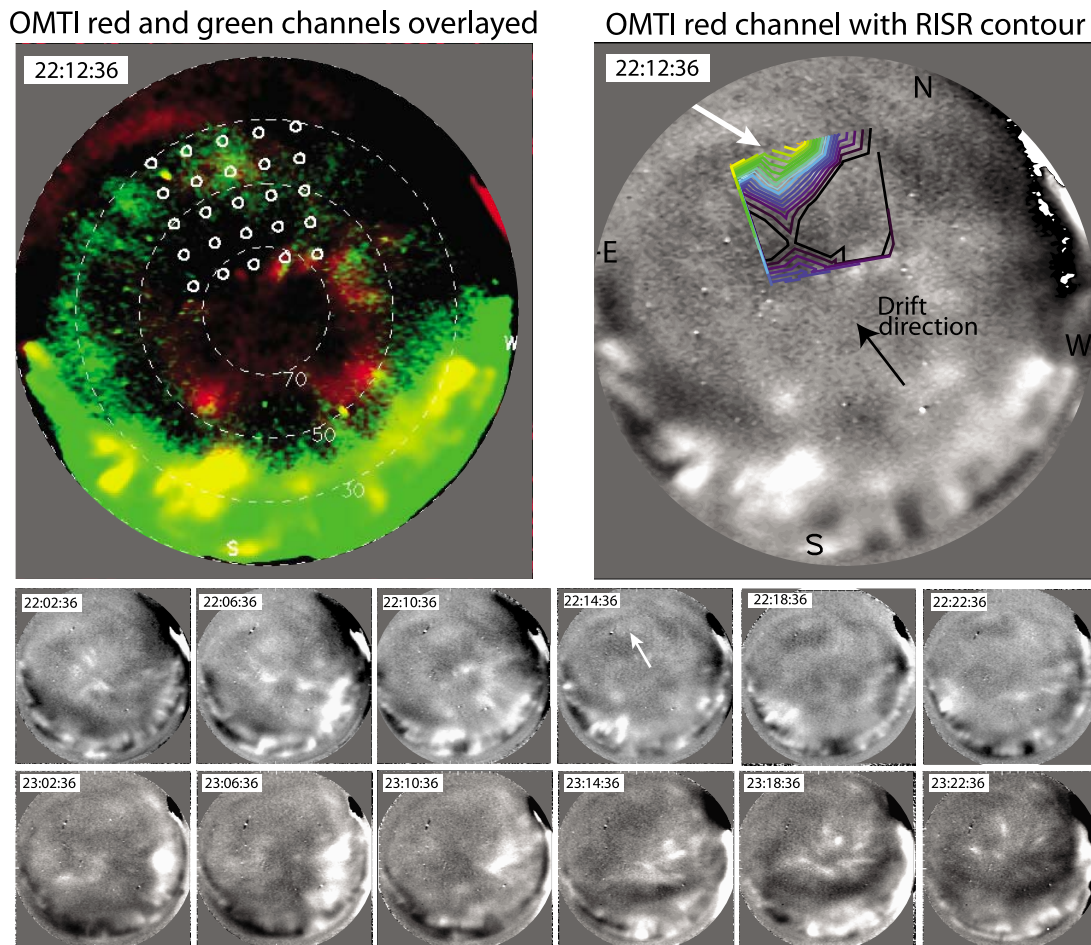
Figure 1. (top left) The radar beam configuration for the RISR-N experiment on 11 December 2011 (white small circles), superimposed on an color-coded overlay of the OMTI 630.0 nm all-sky image (red) and 557.7 nm image (green), taken at 22:12:36 UT. The larger circles mark the elevation angle in degrees. (top right) OMTI 630.0 nm all-sky image, with the integrated RISR-N contours overplotted. The white arrow indicates the plasma structure discussed further in the text, and the black arrow shows the direction of the drift of the structures. (middle) A sequence of OMTI red channel images around the time of the patch, with the patch indicated in the 4th image. (bottom) Images are taken one hour later, and illustrate how the longitudinally extended emission bands break up as they are convected across the FOV of the all-sky imager.

grid pattern shown as white circles in Figure 1 (top left) on a pulse-to-pulse basis, resulting in simultaneous multi-beam measurements when integrating the data over seconds or more. For the data presented in this paper, the measurements were analyzed at 1-minute resolution. At F-region altitudes of $\sim$300 km, the beam pattern covers a horizontal area of roughly 300×400 km. The polar cap plasma structures observed in this study have diameters perpendicular to the geomagnetic field on the order of 100 km, and drift with the convection velocity of a few hundred m/s. It takes such a structure on the order of 10 minutes to drift through the RISR-N field of view (FOV), for which the chosen temporal resolution of one minute is adequate.

[6] Co-located with RISR-N is one of the airglow all-sky imagers of the OMTI system (Optical Mesosphere Thermosphere Imagers) developed by the Solar-Terrestrial Environment Laboratory, Nagoya University [*Shiokawa et al.*, 1999; *Hosokawa et al.*, 2006]. The OMTI camera captures images in 630.0 nm every two minutes with an exposure time of 30 s. A one-hour running average is subtracted from each 630.0 nm image for increased contrast.

30 s exposures in 557.7 nm are also made regularly, but due to gaps in the imaging sequence of this emission, no one-hour average can be removed.

[7] The data discussed here were captured during a radar campaign spanning a few days of very quiet (Kp = 0) conditions in December 2009. At 18 UT (12:15 MLT) on 11 December, the z-component of the interplanetary magnetic field, IMF B_z, turned southward, and remained negative during a period of a few hours, together with negative B_y and positive B_x components. During this time, structured faint plasma enhancements were detected in the RISR-N beams (SNR of only 0–3 dB at the peak of the enhancements), drifting anti-sunward in the north-eastward direction. Clear skies made optical observations with the OMTI imager possible on this night.

3. Results and Discussion

[8] Figure 2 shows a volumetric image of a plasma density structure in the dayside F region polar cap ionosphere at 22:13 UT on 11 December 2009. The figure is created by a
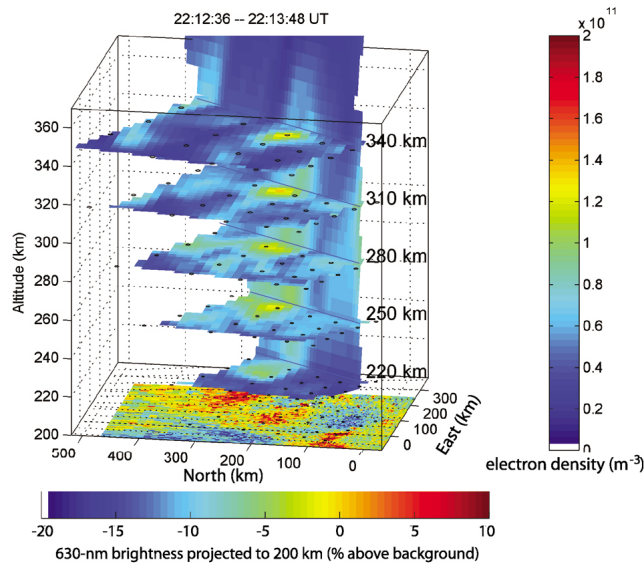
Figure 2. Volumetric image of an F region plasma density structure in the polar cap, created from interpolated RISR-N data captured on 11 December 2009 at 22:12:36–22:13:46 UT. The horizontal slices show the electron density at 220, 250, 280, 310 and 340 km altitude. The contemporary 630.0 nm all-sky image is projected onto the 200 km plane. The locations of the radar beams at each altitude slice are indicated as black circles.

three dimensional linear interpolation of the electron density measurements onto a regular Cartesian grid, from which horizontal slices are extracted at the selected altitudes indicated in the figure. A similar technique was used by *Nicolls et al.* [2007] for measurements in the F-region and by *Semeter et al.* [2009] for auroral E-region. A vertical slice that connects the planes is also displayed in Figure 2 and the resulting image shows a relatively weak but coherent structure, of roughly $100 \times 100 \times 100$ km size. The background-corrected, contemporary OMTI 630.0 nm all-sky image is projected to 200 km altitude (for visualization purposes, the peak altitude of the emission is assumed to be ~250 km), and the color bar indicate the emission brightness in percent over the subtracted background. The positions of the radar beams are superimposed on each layer. The OMTI all-sky imagers show faint emissions, with brightnesses in 630.0 nm of up to 300 R and in 557.7 nm of up to 50 R during the few hours of observed plasma enhancements in the radar data. An overlaid false color (557.7 nm in green, 630.0 nm in red) image is displayed in Figure 1 (top left). The background airglow was subtracted from the green channel by fitting the van Rhijn function to the image, that is, correcting the image for the longer viewing path through the airglow layer at lower elevation angles. The bright region in the south is the poleward edge of the auroral oval. When the structures pass straight overhead the OMTI imager, their horizontal shapes are predominantly round or oval, with diameters down to about 20 km, if assuming an emission altitude of 250 km. Figure 1 (top right) shows the 630.0 nm data for the same time, where RISR-N data integrated along each beam are overlaid as a contour plot. The structure monitored in the radar data in Figure 2 is the enhancement indicated with an arrow, which can be discerned as faint emissions in both the

green and the red OMTI channels, and a sequence of red channel images around this time is displayed in Figure 1 (middle), with the structure indicated with an arrow in the 4th image. Rayed structures of the emissions along the geomagnetic field can often be seen when they are off zenith, with the higher altitude red emission closer to the center of the image than the green 557.7 nm emission, due to perspective effects. This effect may indicate the presence of soft particle precipitation. For the structure of interest in this study, such evidence of precipitation could not be established solely from the optical data.

[9] The plasma structures are drifting in the north-eastward (anti-sunward) direction throughout the time period of southward IMF B_z. The drift velocity is derived from the all-sky data to be 300 m/s at the start of the interval and then increase somewhat. The plasma motion was also computed independently from the radar Doppler measurements, by utilizing the inversion technique described by *Semeter et al.* [2010] and *Butler et al.* [2010]. Figure 3 (top) shows the evolution of the structure over time, from electron density contours at 270 km altitude. The estimated drift of the center of the structure in the first panel is calculated from the Doppler measurements and illustrated as a black star in each image, with the drift history plotted in blue. A good correspondence is found between the relocalization of the enhancement and its estimated Doppler drift. The observed north-east flow field agrees with earlier studies showing auroral transients moving eastward in the northern hemisphere for negative IMF B_y during periods of southward IMF B_z [*Moen et al.*, 1995].

[10] The altitude variation of the structure is examined by taking a vertical slice through the three dimensional volume for the selected times (Figure 3, middle). The slice is a north-south cut taken through the center of the enhancement, indicated with black lines in Figure 3 (top). At 22:11:21 UT the peak of the electron density occurs at about 260 km altitude. In the next minute, the enhancement has decayed and shifted upwards, with the density peak at 340 km. However, in the subsequent minute, at 22:13:51 UT, the electron density of the plasma structure has increased again, at the same time as the altitude of the peak is found at about 280 km. The structure then decays again as it drifts north-east (rightmost panel, data from 22:17:33 UT). Figure 3 (bottom) shows the contemporary volumetric images of the described evolution, where the plots are of the same format as in Figure 2. Line plots of the weighted average of the electron density within the plasma structure as a function of altitude are shown in Figure 4 (left), for the three first time intervals discussed in Figure 3. The horizontal dashed lines mark the associated standard deviation. It is clear that the largest observed electron density takes place at 22:13:51 UT (green profile), with a peak close to 280 km altitude. The volumetric images show now indication of a second large plasma structure drifting into this structure at this time. The density increase by about 10^{10} m^{-3} between profiles 2 and 3 at this altitude is of the same order as found in the ionospheric chemistry model results by *Weber et al.* [1989] after 1 minute of soft precipitation. The data thus suggest that low energy precipitation is present, as the structure is following the plasma convection to the north-east. However, the ratios of electron and ion temperature at the same times are shown in Figure 4 (right), where no clear heating can be seen at the time of increased plasma density. If auroral ionization is
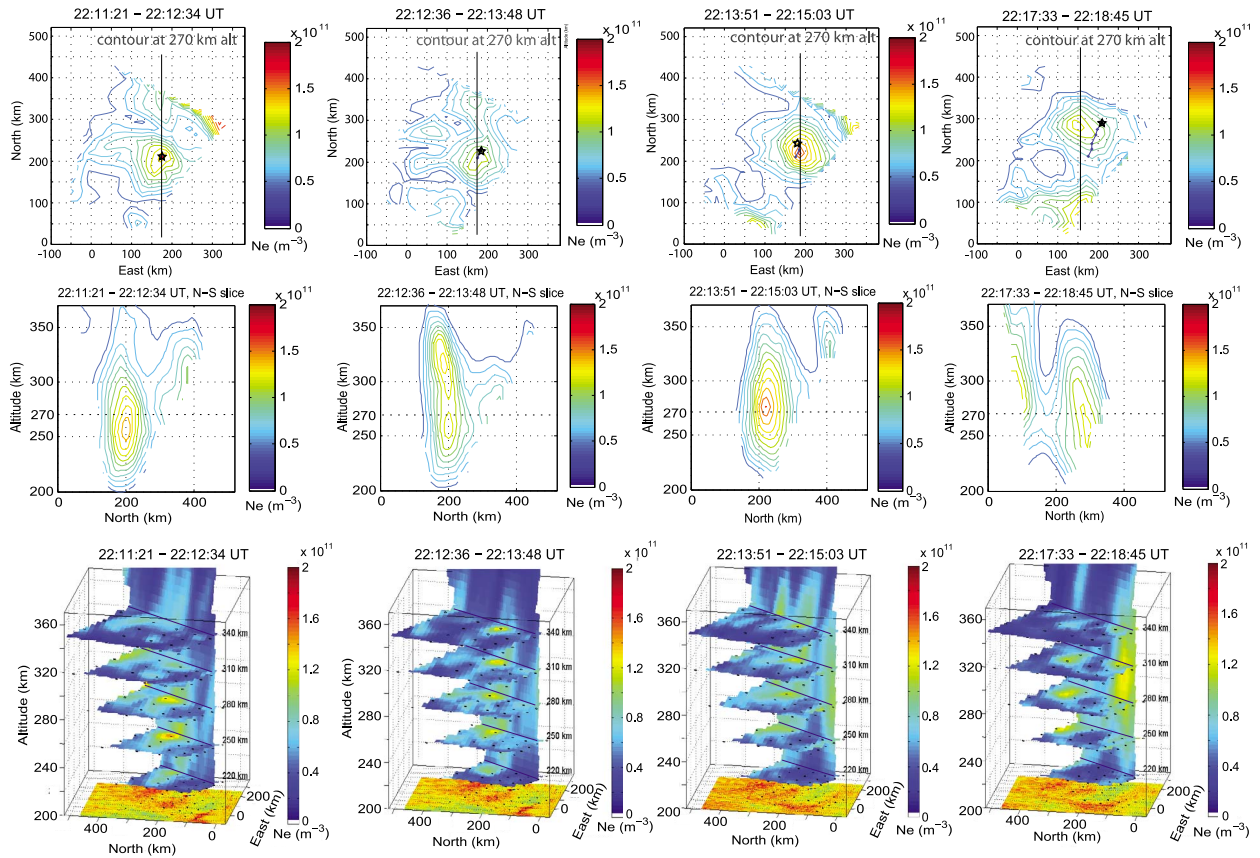
Figure 3. (top) Contour plots made from a slice at 270 km altitude, showing the temporal evolution of a plasma irregularity as it drifts across the radar FOV. The black stars mark the position of the center of the structure as estimated from the Doppler shift measurements. (middle) Position of the cut to create the vertical contour plots denoted by the black line in Figure 3 (top). (bottom) The volumetric images for the sequence, in the same format as in Figure 2.

present, there should be an increase of electron temperature above the structure [e.g., *Zettergren et al.*, 2007], which is not seen. To resolve this apparent discrepancy, the time history of the flux tubes needs to be modeled and understood. It is possible that if the structure is built up slowly over time due to a very low number flux of soft particles, the electron temperature may not be enhanced. A comprehensive model is needed to parse the various production and loss terms of
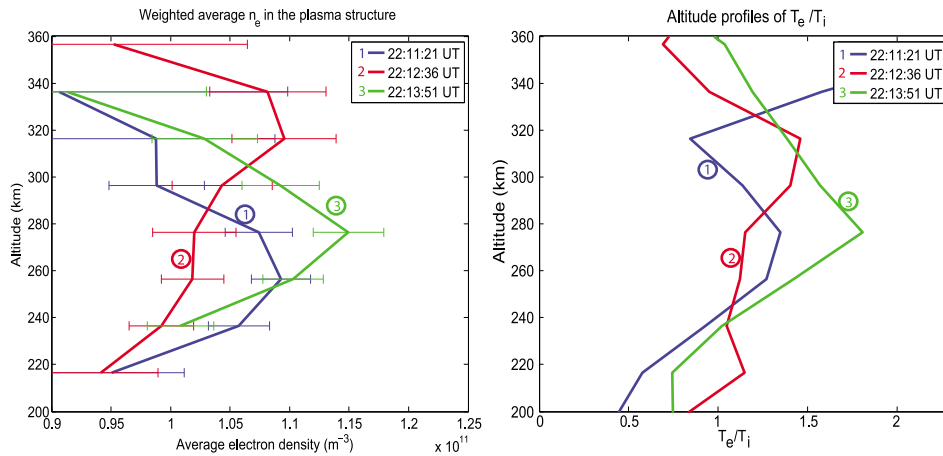
Figure 4. (left) Time evolution of the average altitude profiles of the electron density of the plasma structure shown in Figure 3. The density decreases at 280 km altitude between times 1 and 2 but gets enhanced at 330 km, which is an indication of low energy precipitation at the time. In time step 3 the density increases again at 280 km, after which the whole structure fades again. The density is calculated from the weighted average of the electron density of the plasma structure in each horizontal plane. The dashed lines show the standard deviation associated with the average. (right) Temperature ratios for the same times.
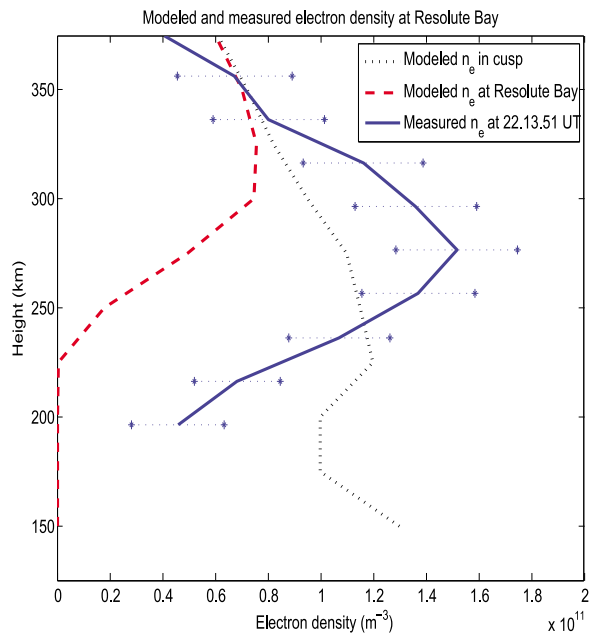
Figure 5. Modeled typical electron density profile in the cusp (black, dotted line) from the TRANSCAR model. As the patch drifts anti-sunward toward Resolute Bay, recombination of the electrons with molecular species will cause the profile to decrease to the red, dashed line. The blue line shows the measured electron density profile of the plasma structure discussed in this paper, at 22:13:51 UT. The larger density and lower peak could indicate the presence of electron precipitation, although electron densities in the cusp are known to be highly variable.

the electron continuity equation and to draw any firm conclusions about precipitation, which is beyond the scope of this letter.

[11] A patch forming in the cusp region will decay as it drifts anti-sunward, due to recombination of the electrons with foremost N_2 and O_2. A typical density profile in the cusp was modeled with the TRANSCAR model by *Vontrat-Reberac et al.* [2001] and is shown in Figure 5 (black dotted plot). The distance from the cusp to Resolute Bay is estimated to 800 km, and with a drift velocity of about 350 m/s, it would take the structure 38 min to reach Resolute Bay. During this time, the density will have decayed to the red, dashed profile in Figure 5, by using the decay parameter β derived by *Hosokawa et al.* [2011]. This rudimentary model indicates that the measured profile (blue, solid plot) in the figure is likely to originate at least partially from local precipitation, to account for the magnitude of the electron density, the smaller scale height of the measured profile than the modeled, and the lower altitude of the peak.

[12] The plasma transients studied here take place during the daytime hours at Resolute Bay, in the polar cap region just poleward of the cusp. At 22 UT the atmosphere is sunlit above 200 km altitude, so that photoionization by the sun will also impact the electron density in the F region.

[13] The prevailing IMF conditions are favorable for the occurrence of PMAFs due to repeated FTEs. Longitudinally extended bright emission bands are seen to form in the all-sky imagers at the location of the open/closed field line boundary, to the south-west of Resolute Bay, with a

few (4 − 8) minutes intervals, and as they convect to northeast they are broken up into smaller structures of oval or round shape, which can be seen in the sequence of images from 20 minutes of data displayed in Figure 1 (bottom). The emission brightnesses in 630.0 nm and 557.7 nm are characteristic for polar cap patches, with a decreasing I(557.7)/I(630.0) emission ratio from 30% to 10% during the passage of the patches across the all-sky FOV.

4. Summary and Conclusions

[14] The volumetric imaging capability of the ionospheric state parameters (electron density, electron and ion temperature and ion drift) provided by RISR-N can for the first time give detailed information on the three-dimensional temporal and spatial evolution of plasma structures in the polar cap, and allow measurements in the rest frame of the plasma enhancements. Our technique contributes several critical new constraints for understanding polar ionospheric structuring:

[15] 1. Tracking the apparent motion of the ionization structure. The motion could be due to plasma drift or motion of the ionizing source, or both. This can be compared with independent measurements of convection.

[16] 2. Observing changes in the plasma state (T_e, T_i, n_e profiles) in the rest frame of this apparent motion.

[17] 3. Direct comparison of plasma state inside and outside the structure.

[18] 4. Quantifying the evolving geometry (width, height) of the plasma feature.

[19] From combined optical and RISR-N measurements a better understanding of the polar cap ionosphere can be reached, but we need more comprehensive modeling and measurements to fully exploit the information obtained.

References

Bahcivan, H., R. Tsunoda, M. Nicolls, and C. Heinselman (2010), Initial ionospheric observations made by the new Resolute incoherent scatter radar and comparison to solar wind IMF, *Geophys. Res. Lett.*, *37*, L15103, doi:10.1029/2010GL043632.

Basu, S., S. Basu, P. K. Chaturvedi, and C. M. Bryant Jr. (1994), Irregularity structures in the cusp/cleft and polar cap regions, *Radio Sci.*, *29*, 195–207.

Butler, T. W., J. Semeter, C. J. Heinselman, and M. J. Nicolls (2010), Imaging F region drifts using monostatic phased-array incoherent scatter radar, *Radio Sci.*, *45*, RS5013, doi:10.1029/2010RS004364.

Fasel, G. J. (1995), Dayside poleward moving auroral forms: A statistical study, *J. Geophys. Res.*, *100*, 11,891–11,905.

Hosokawa, K., K. Shiokawa, Y. Otsuka, A. Nakajima, T. Ogawa, and J. D. Kelly (2006), Estimating drift velocity of polar cap patches with all-sky airglow imager at Resolute Bay, Canada, *Geophys. Res. Lett.*, *33*, L15111, doi:10.1029/2006GL026916.

Hosokawa, K., K. Shiokawa, Y. Otsuka, T. Ogawa, J.-P. St-Maurice, G. J. Sofko, and D. A. Andre (2009), Relationship between polar cap patches and field-aligned irregularities as observed with an all-sky airglow imager at Resolute Bay and the PolarDARN radar at Rankin Inlet, *J. Geophys. Res.*, *114*, A03306, doi:10.1029/2008JA013707.

Hosokawa, K., J. I. Moen, K. Shiokawa, and Y. Otsuka (2011), Decay of polar cap patch, *J. Geophys. Res.*, *116*, A05306, doi:10.1029/2010JA016297.

Lorentzen, D. A., J. Moen, K. Oksavik, F. Sigernes, Y. Saito, and M. G. Johnsen (2010), In situ measurement of a newly created polar cap patch, *J. Geophys. Res.*, *115*, A12323, doi:10.1029/2010JA015710.

Milan, S. E., M. Lester, S. W. H. Cowley, J. Moen, P. E. Sandholt, and C. J. Owen (1999), Meridian-scanning photometer, coherent HF radar, and magnetometer observations of the cusp: A case study, *Ann. Geophys*, *18*, 159–172.

Moen, J., P. E. Sandholt, M. Lockwood, W. F. Denig, U. P. Løvhaug, B. Lybekk, A. Egeland, D. Opsvik, and E. Friis-Christensen (1995), Events of enhanced convection and related dayside auroral activity, *J. Geophys. Res.*, *100*, 23,917–23,934.

Nicolls, M. J., C. J. Heinselman, E. A. Hope, S. Ranjan, M. C. Kelley, and J. D. Kelly (2007), Imaging of polar mesosphere summer echoes with the 450 MHz Poker Flat Advanced Modular Incoherent Scatter Radar, *Geophys. Res. Lett.*, *34*, L20102, doi:10.1029/2007GL031476.

Oksavik, K., V. L. Barth, J. Moen, and M. Lester (2010), On the entry and transit of high-density plasma across the polar cap, *J. Geophys. Res.*, *115*, A12308, doi:10.1029/2010JA015817.

Russell, C. T., and R. C. Elphic (1978), Initial ISEE magnetometer results: Magnetopause observations, *Space Sci. Rev.*, *22*, 681–715.

Sandholt, P. E., M. Lockwood, T. Oguti, S. W. H. Cowley, K. S. C. Freeman, B. Lybekk, A. Egeland, and D. M. Willis (1990), Midday auroral breakup events and related energy and momentum transfer from the magnetosheath, *J. Geophys. Res.*, *95*, 1039–1060.

Sandholt, P. E., and C. J. Farrugia (2007), Poleward moving auroral forms (PMAFs) revisited: Responses of aurorae, plasma convection and Birkeland currents in the pre- and postnoon sectors under positive and negative IMF B$_y$ conditions, *Ann. Geophys.*, *25*, 1629–1652.

Semeter, J., T. Butler, C. Heinselman, M. Nicolls, J. Kelly, and D. Hampton (2009), Volumetric imaging of the auroral ionosphere: Initial results from PFISR, *J. Atmos. Sol. Terr. Phys.*, *71*, 738–743.

Semeter, J., T. W. Butler, M. Zettergren, C. J. Heinselman, and M. J. Nicolls (2010), Composite imaging of auroral forms and convective flows during a substorm cycle, *J. Geophys. Res.*, *115*, A08308, doi:10.1029/2009JA014931.

Shiokawa, K., Y. Katoh, M. Satoh, M. K. Ejiri, T. Ogawa, T. Nakamura, T. Tsuda, and R. H. Wiens (1999), Development of optical mesosphere thermosphere imagers (OMTI), *Earth Planets Space*, *51*, 887–896.

Tsunoda, R. T. (1988), High-latitude F region irregularities: A review and synthesis, *Rev. Geophys.*, *26*, 719–760.

Vasyliūnas, V. M., and P. Song (2005), Meaning of ionospheric Joule heating, *J. Geophys. Res.*, *110*, A02301, doi:10.1029/2004JA010615.

Vontrat-Reberac, A., D. Fontaine, P.-L. Blelly, and M. Galand (2001), Theoretical predictions of the effect of cusp and dayside precipitation on the polar ionosphere, *J. Geophys. Res.*, *106*, 28,857–28,874.

Weber, E. J., J. Buchau, J. G. Moore, J. R. Sharber, R. C. Livingston, J. D. Winningham, and B. W. Reinisch (1984), F layer ionization patches in the polar cap, *J. Geophys. Res.*, *89*, 1683–1694.

Weber, E. J., et al. (1989), Rocket measurements within a polar cap arc: Plasma, particle, and electric circuit parameters, *J. Geophys. Res.*, *94*, 6692–6712.

Zettergren, M., J. Semeter, P.-L. Blelly, and M. Diaz (2007), Optical estimation of auroral ion upflow: Theory, *J. Geophys. Res.*, *112*, A12310, doi:10.1029/2007JA012691.

T. W. Butler, H. Dahlgren, and J. L. Semeter, Department of Electrical and Computer Engineering, Boston University, 725 Commonwealth Ave., Boston, MA 02215, USA. (hannad@bu.edu)

C. Heinselman and M. J. Nicolls, SRI International, 333 Ravenswood Ave., Menlo Park, CA 94025, USA.

K. Hosokawa, Department of Communication Engineering and Informatics, University of Electro-Communications, Chofugaoka 1-5-1, Chofu, Tokyo 182-8585, Japan.

M. G. Johnsen, Tromsø Geophysical Observatory, University of Tromsø, N-9037 Tromsø, Norway.

K. Shiokawa, Solar-Terrestrial Environment Laboratory, Nagoya University, Furo-cho, Chikusa-ku, Nagoya, Aichi 464-8601, Japan.